

Constrained Deep Reinforcement Based Functional Split Optimization in Virtualized RANs

Fahri Wisnu Murti, Samad Ali, and Matti Latva-aho

Centre for Wireless Communications, University of Oulu, Finland

Abstract

Virtualized Radio Access Network (vRAN) brings agility to Next-Generation RAN through *functional split*. It allows decomposing the base station (BS) functions into virtualized components and hosts it either at the distributed-unit (DU) or central-unit (CU). However, deciding which functions to deploy at DU or CU to minimize the total network cost is challenging. In this paper, a constrained deep reinforcement based functional split optimization (CDRS) is proposed to optimize the locations of functions in vRAN. Our formulation results in a combinatorial and NP-hard problem for which finding the exact solution is computationally expensive. Hence, in our proposed approach, a policy gradient method with Lagrangian relaxation is applied that uses a penalty signal to lead the policy toward constraint satisfaction. It utilizes a neural network architecture formed by an encoder-decoder sequence-to-sequence model based on stacked Long Short-term Memory (LSTM) networks to approximate the policy. Greedy decoding and temperature sampling methods are also leveraged for a search strategy to infer the best solution among candidates from multiple trained models that help to avoid a severe suboptimality. Simulations are performed to evaluate the performance of the proposed solution in both synthetic and real network datasets. Our findings reveal that CDRS successfully learns the optimal decision, solves the problem with the accuracy of 0.05% optimality gap and becomes the most cost-effective compared to the available RAN setups. Moreover, it is seen that altering the routing cost and traffic load does not significantly degrade the optimality performance. The results also show that all of our CDRS settings have faster computational time than the optimal baseline solver. Our proposed method fills the gap of optimizing the functional split offering a near-optimal solution, faster computational time and minimal hand-engineering.

Index Terms

Virtualized RANs, Functional Split, Optimization, Neural Network, Deep Reinforcement Learning

A preliminary version of this work appears in IEEE ICC 2021 Workshop [1]. This work was supported by the Academy of Finland 6Genesis Flagship (grant no. 318927).

I. INTRODUCTION

The increase in mobile data traffic of emerging applications with diverse requirements has driven the efforts to re-design the radio access networks (RANs). There have been systematic works in standardization bodies to adopt the concept of *softwarization* and *virtualization* to the RAN architecture [2]–[4]. Cloud/Centralized-RAN (C-RAN) has become a favorable solution to enable the low-cost deployment and high-performance systems by pooling the baseband functions of the base station (BS) to a central server which is also known as Cloud/Central Unit (CU). Through a centralized control, such approach can offer cost-efficient solution and high-performance network management simultaneously in RANs. However, a fully centralized RAN faces many challenging issues. For instance, it requires a low-latency and high capacity fronthaul which are often not available in current RANs and costly to build from scratch. Such challenges motivate the shift of rigid C-RAN to flexible architectures where a subset of BS functions is hosted at CU and the other functions are at distributed units (DUs).

The term *virtualized RAN* (vRAN)¹ is used to describe an architecture that allows deploying different *functional split* options for each BS [2]–[4]. Functional split is a protocol stack disaggregation that enables decomposing the BS functions into virtualized components (except RF unit) and hosts it either at DU or CU. It brings flexibility to the network by placing BS functions at different places by considering aspects such as traffic demand, network cost and locations. Selecting a functional split configuration (which functions to deploy at CU and functions at the DU) for each BS is essential. It allows to identify how efficient this decomposition and which requirements must be satisfied. However, it is also a challenging problem because each split differs in delay requirements, initiates different computation loads for CU and DU, and creates different data flows. There is also a consent that the initial design using an evolved Common Public Radio Interface (eCPRI)/CPRI should be replaced by Integrated Backhaul/Fronthaul (Crosshaul) based on an open interface and packet-switch (shared) network which is more cost-efficient [5], [6]. As a result, functional split requires a careful design, especially in such a shared link with a limited capacity. These issues testify that optimizing the split configuration is vital, although it may increase RAN management's complexity. Otherwise, an unoptimized function split can lead to inefficient RANs and even to performance degradation [7].

¹The CU and DU to be run as a virtualized software, e.g., virtual CU (vDU) and virtual CU (vCU), in different computing device. A far-edge server is typically for vDU deployment while vCU is in a more centralized server. O-RAN Alliance (<https://www.o-ran.org/>) also defines the term O-CU and O-DU for the respective entities.

A. Related Works

3GPP [2], [3] and a seminal white paper [4] have defined the detail vRAN split specifications. Although the authors in [8] have discussed the gains and requirements of the vRAN split, there are still limited works on the optimization issues. Energy consumption for various splits has been evaluated in [9], then the authors have proposed an optimization model over different splits. The authors in [6] studied optimizing the centralization degree of C-RAN/vRAN over Crosshaul. Follow-up works, [10] and [11] offered an optimal solution of minimizing total cost for integration vRAN with Mobile Edge Computing (MEC). Then, [12] proposed an optimized multi-cloud vRAN framework with balancing its centralization [7]. The authors in [13] proposed the PlaceRAN framework to minimize the computing resources while maximizing the radio functions aggregations which relies on a commercial solver, e.g., IBM CPLEX, to find the optimal solution. These mentioned works [6], [7], [9]–[13] have addressed various vRAN problems but still rely on the mathematical model and intuitive heuristic algorithm design to define their problems' structure. Such approaches require prior knowledge of problem expertise (e.g., formulating each problem mathematically) that may not be possible in practice [14]. Additionally, it needs heavy mathematical solutions that often have exponential complexity and slow execution time particularly in large networks. The above problems are also often complex combinatorial and difficult to solve. Hence, we opt out to use optimization-based approaches to tackle the functional split problem in vRAN.

In operational research, *machine learning* (ML) approaches have spurred to address combinatorial optimization problems without much hand-engineering and heuristic algorithm design [14]. It becomes an alternative solution to tackle an NP-hard problem, where the exact algorithm is computationally expensive. One exciting idea is enumerating an input and output of an optimization problem and building it into a dataset. This dataset is then utilized for training ML models such as neural networks. Then, we can use the trained neural network to predict the output from a specific input. The authors in [15] have built supervised learning based on pointer networks (Ptr-Nets) and successfully demonstrated to find the near-optimal solution on Traveling Salesman Problem (TSP). However, this approach still requires access to optimal labels that may not be possible in many problems. To this end, Bello *et al* proposed *Neural Combinatorial Optimization* (NCO) framework with an end-to-end approach via neural network and *reinforcement learning* (RL) to tackle this limitation [16]. Instead of directly accessing the optimal label, it uses some reward feedbacks to a learning algorithm and a verifier to assess the quality of a set of solutions.

Once the model is trained, we can use it to solve the optimization problem inexpensively and quickly. This framework has successfully solved combinatorial problems in operational research offering a near-optimal solution, minimal hand-engineering and fast execution time, e.g., TSP, 0-1 Knapsack problem [16], Job Shop Scheduling (JSP) [17], device placement problem [18], and vehicle routing problem [19]. This approach is promising in solving complex combinatorial problems for zero-touch optimization in wireless network [20], [21]. However, there is still limited works to employ it for network management problems particularly addressing functional split optimization in vRAN [22].

The NCO framework with RL have been studied by Jiang *et al.* to solve the offloading problem in MEC and showed that their approach attained more than 98% of optimality [23]. The authors in [24] also proposed similar framework with constrained deep RL and sequence-to-sequence model to solve the virtual network function (VNF) placement problem and aimed to minimize the power consumption. In vRAN, the authors in [25] proposed a vrAIn framework that utilizes a deep RL paradigm for dynamic computing and radio resources control. However, none of these works [23]–[25] discuss ML approaches, specifically deep RL, to address functional split problem in vRAN. Recent work in [26] has studied user-centric network slicing and the functional split problem with deep learning architecture. The proposed framework is based on supervised learning that relies on high-quality labelled datasets (e.g., optimal labels). In this case, the problem is defined mathematically as integer linear programming (ILP), then solve the multiple instances of the problem using a commercial solver (e.g., IBM CPLEX) to generate the datasets. The datasets are then trained via a deep learning architecture. Once trained, the model can be used quickly in an online manner offering a real-time solution. Despite the approach in [26] is interesting, it still needs to define the problem mathematically to construct high-quality labels that are often inaccurate in practice. Instead of following approach in [26], we leverage NCO framework with constrained deep RL to address functional split optimization with minimal hand-engineering. To the best of our knowledge, this is the first work using constrained deep RL paradigm to solve the functional split problem in the vRAN system.

B. Methodology & Contributions

Our goal is to develop a zero-touch optimization framework that optimizes the functional split configuration decision for each BS in a vRAN system. First, we formulate and present the functional split problem mathematically to provide a better understanding of its objective

and constraints. Our formulation results in a combinatorial and NP-hard problem. Therefore, it is computationally expensive to solve optimally, especially for large-scale networks and real-time execution. Moreover, solving such a problem often relies on the problem expertise (e.g., mathematical model, heuristic algorithm design) that may also be insufficient in practice.

Motivated by recent works in NCO with RL approach [16], [17], [24], we formulate the functional split problem above as *constrained neural combinatorial reinforcement learning* and develop a *constrained deep RL based functional split optimization (CDRS)* framework for solving the problem. We use neural networks to map the state observations to the actions. The CDRS’s idea is to estimate the neural network model’s parameters iteratively by taking instances from the problem spaces using a deep RL paradigm. Hence, for every interaction with the environment (vRAN system), we expect to receive a reward (total network cost) and a penalty signal (constraints violation) and the output returned by the neural network to learn and improve the model. It is worth noting that our approach requires minimal hand-engineering. Our approach does not need to know the problem mathematically, e.g., mathematical optimization, or direct access to the optimal labelled data, e.g., supervised learning. Instead, it learns from interaction with the environment.

CDRS framework follows constrained deep RL paradigm based on constrained policy optimization and neural network architecture to train the model. It is tailored from a Policy Gradient [27] with Lagrangian relaxation method [28]. Besides the reward (total network cost) signal, it expects to receive penalization feedback for every constraint violation that guides the policy toward constraint satisfaction. Since deciding the penalty coefficient (Lagrange multiplier) is a multi-objective problem, we apply two following settings: 1) *CDRS-Fixed* that manually selects and uses a fixed penalty coefficient (reward shaping) [17], [24]; and, a less intuitive selection, 2) *CDRS-Ada* that adaptively updates the penalty coefficient in the ascent direction [29]. It also uses a neural network to approximate the policy, formed by an encoder-decoder sequence-to-sequence model [30], [31] based on stacked Long Short Term Memory (LSTM) networks. Also, a baseline estimator is separately trained in an auxiliary network to improve the policy further. Once the model is trained, finding the solution for the problem is computationally efficient as it only requires a forward pass through the trained neural network. Hence, we include two different strategies to infer the best solution among multiple candidates [16]. By considering candidates from multiple trained models, this helps to reduce the inferred policy suffering from a severe suboptimality. Firstly, we use a greedy decoding method, e.g., *CDRS-Fixed-G* and *CDRS-Ada-*

G , that selects the function split configuration with the largest probability for having the lower cost. Secondly, we apply a sampling method with a temperature hyperparameter (temperature sampling), e.g., *CDRS-Fixed-T* and *CDRS-Ada-T*. It samples the multiple candidate solutions from the stochastic policy for every trained model before deciding which one is the best solution with the lowest total cost.

We conduct several experiments to evaluate the CDRS framework in terms of training behaviour, optimality performance, the impact of altering the traffic load and routing cost and the computational time. We evaluate the CDRS framework in a synthetic network generated by the Waxman algorithm that highly represents a backhaul network [32] and a real network dataset from [33]. The used system parameters are from a measurement-based 3GPP-compliant system model [7], [12]. To assess the effectiveness of our approach, we compare it to the optimal value obtained from a Python-MIP solver². Following our evaluations, CDRS framework successfully learns the optimal function split decision and solves the problem with 0.05% optimality gap³ (e.g., CDRS-Fixed-T). CDRS’s optimality performance also does not significantly degrade with altering the routing cost and traffic load. Our results also show that CDRS is the most cost-effective compared to two extreme cases: fully C-RAN and D-RAN. In terms of computational time, all of our CDRS settings are faster than MIP Solver where CDRS-Ada-G can attain as high as 22.82 times faster. Our findings also reveal that CDRS-Fixed-T has the least optimality gap while CDRS-Ada-G has the fastest computational time. Our contributions can be summarized:

- **New problem formulation.** We formulate the vRAN split problem to *constrained neural combinatorial reinforcement learning* which can be solved with minimal hand-engineering.
- **Novel solution approach.** We propose a CDRS framework as a solution approach. It is tailored from a constrained policy optimization with self-competing baseline estimator and uses a neural network architecture formed by an encoder-decoder sequence-to-sequence model with stacked LSTM. Following the CDRS framework, we propose four settings depending on the penalty coefficient updates and search strategies: CDRS-Fixed-G, CDRS-Fixed-T, CDRS-Ada-G and CDRS-Ada-T. CDRS does not need to know the problem mathematically or directly access the optimal labelled data; instead, it learns from interaction with the environment. Once the model is trained, finding the solution is fast and inexpensive.

²We use a solution obtained from a mixed-integer programming solver (<https://www.python-mip.com/>) as an optimal baseline comparison. It offers an exact solution through a well-known method, Branch-&-Cut algorithm.

³We use the term *optimality gap* to define our solution’s error compared to the optimal value obtained from MIP Solver.

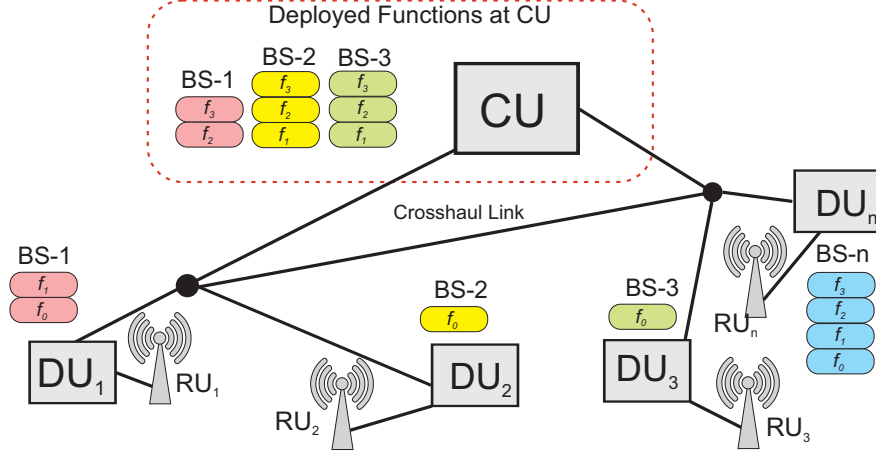


Fig. 1: vRAN over integrated backhaul/fronthaul. It has many degrees of design freedom by possibly hosting BS functions at CU or DU.

- We conduct a series of experiments with 3GPP-compliant parameters in a synthetic network generated by the Waxman algorithm and a real network dataset. We investigate the training behaviour, the accuracy of the solution, the impact of routing cost and traffic load and the computational time.

The rest of this paper is organized as follows. The background and system model of vRAN are presented in Section II. The functional split problem is formalized mathematically in Section III. Our proposed framework is described in Section IV. Our simulation and experiment results are discussed in Section V. Finally, our work is concluded in Section VI.

II. SYSTEM MODEL

Background. In C-RAN, all BS functions are at Base Band Unit (BBU) except RF layers at Radio Unit (RU). In the development, BBU functions are decoupled into CU and DU [3]. Hence, a BS consists of CU, DU and RU. Fig 1 shows that a CU is typically a bigger server and placed in a central location, while DU is smaller and located near (or co-located) with RU.

Our model refers to the standardization of 3GPP [2], [3] and seminal white paper [4], where each split has a different performance gain [7], [8]. **Split 0:** All functions are at DU except the RF layer is at RU. It is a typical D-RAN setup. **Split 1 (PDCP-RLC):** RRC, PDCP, and upper layers are hosted at CU, while RLC, MAC, and PHY are at DU. It enables L3 and L2 operation at the same server. **Split 2 (MAC-PHY):** MAC and upper layers are at CU; PHY at DU. It allows improvement for CoMP by centralized HARQ. **Split 3 (PHY-RF):** All functions are at CU, except

Split Options	Flow (Mbps)	Delay Req. (ms)
0	λ	30
1	λ	30
2	$1.02\lambda + 1.5$	2
3	2500	0.25

TABLE I: Data and delay requirements of vRAN split when the traffic load is λ Mbps [10], [11].

RF layers. It is a fully centralized version of vRAN, and gains power-saving and improved joint reception CoMP with uplink PHY level combining. Going from Split 1 to 3, more functions are hosted at CU. In addition to increasing network performance, a higher centralization level can lead to more cost-saving [7]. However, centralizing more functions increases the data load to be transferred to CU, going from λ in S0 to 2.5 Gbps in S3 for each BS, and has stricter delay requirements. Table I describes the particular vRAN split options and their requirements.

RAN. We model a vRAN architecture with a graph $G = (\mathcal{I}, \mathcal{E})$ where \mathcal{I} has a subsets \mathcal{N} of the N DUs, routers and a CU (index 0). Each node is connected through a link of (i, j) with a set \mathcal{E} and has capacity c_{ij} (Mbps) each. The DU- n is connected to $\{0\}$ with a single path (e.g., shortest path) p_{n0} ; hence, we define $r_{p_{n0}}$ as the amount of data flow (Mbps) is transferred and routed through path $p_{n0} := \{(n, i_1), \dots, (i_k, 0) : (i, j) \in \mathcal{E}\}$. The BS functions are deployed in servers using virtual machines (VMs). Each server has a processing capacity, i.e., H_n for DU- n and H_0 for CU. Naturally, a central server has a higher computing performance and capacity. We define that $H_0 \geq H_n$ and $\rho_o^c \leq \rho_o^d$, where ρ_o^c and ρ_o^d are the incurred computational load (cycle/Mb/s) in result of deploying the split configuration $o \in \{0, 1, 2, 3\}$ at CU and DU, respectively.

Demand & Cost. We focus on the uplink transmission where λ_n (Mbps) is the aggregate data flow of DU- n to serve the users traffic; hence, there are N different flows in the network. We denote $\alpha = (\alpha_n, n \in \mathcal{N})$ and $\beta = (\beta_n, n \in \mathcal{N})$ as cost for instantiating the VM (monetary units) and the computing cost (monetary units/cycle) at DU- n , respectively, while α_0 and β_0 are the respective cost for CU. We also have a routing cost $\zeta_{p_{n0}}$ (monetary units/Mbps) for each path p_{n0} . This cost arises from the network link are leased from third parties or the expenditures of maintaining the link.

Problem Statement. We have four choices of split configurations for each BS in vRAN. What is the best-deployed split configuration for each BS that minimizes the total network cost? The decision leads to interesting problems. Each configuration generates a different DU-CU data flow and has a distinct delay requirement. Executing more functions at CU is more efficient in

terms of computing cost; however, it produces a higher load of crosshaul links. There is also delay processing and limited capacity for each server and network link. Finally, the goal is to solve this problem with minimal hand-engineering.

III. FORMALIZATION OF VRAN SPLIT PROBLEM

The BS functions can be deployed at DU (for each BS) or pooled at CU according to the split configuration, as seen in Table I. The configuration must respect to the *chain of functions* $f_0 \rightarrow f_1 \rightarrow f_2 \rightarrow f_3$. Thus, we define binary variable x_{on} as the decisions for deploying split $o \in \{0, 1, 2, 3\}$ at DU- n . For instance, $x_{0n} = 1$ is for deploying f_0, f_1, f_2, f_3 (Split 0); $x_{1n} = 1$ for f_0, f_1, f_2 (Split 1); $x_{2n} = 1$ for f_0, f_1 (Split 2); or $x_{3n} = 1$ for f_0 (Split 3) at DU- n . We only deploy a single configuration for each BS. Therefore, the set of eligible split configuration is:

$$\mathcal{X} = \left\{ \mathbf{x}_n \in \{0, 1\} \mid \sum_{o=0}^3 x_{on} = 1, \quad \forall n \in \mathcal{N} \right\}, \quad (1)$$

where $\mathbf{x}_n = (x_{on}, \forall o)$ and $\mathbf{x} = (\mathbf{x}_n, \forall n)$. The BS functions, f_1, f_2 and f_3 , are deployed in servers with VMs at each server. We have computational processing for CU and for each DU that must respect its capacity as:

$$\sum_{n \in \mathcal{N}} \lambda_n \sum_{o=0}^3 x_{on} \rho_o^c \leq H_0, \quad (2)$$

$$\lambda_n \sum_{o=0}^3 x_{on} \rho_o^d \leq H_n, \quad \forall n \in \mathcal{N}. \quad (3)$$

Data Flow & Delay. Variable $r_{p_{n0}}$ (Mbps) defines the amount of data flow (Mbps) are transferred through path p_{n0} . Hence, the flow must respect the link capacities:

$$\sum_{n \in \mathcal{N}} r_{p_{n0}} I_{p_{n0}}^{ij} \leq c_{ij}, \quad \forall (i, j) \in \mathcal{E}, \quad (4)$$

where $I_{p_{n0}}^{ij} \in \{0, 1\}$ indicates whether the link (i, j) is used by path p_{n0} . Assuming a single path (e.g., shortest path) the amount of data flow depending on the split configuration is [10]:

$$r_{p_{n0}} = \lambda_n (x_{0n} + x_{1n}) + x_{2n} (1.02\lambda_n + 1.5) + 2500x_{3n}. \quad (5)$$

Lets denote $d_{p_{n0}}$ is a delay incurred for routing to path p_{n0} from DU- n to CU. Each split configuration has to satisfy the respective delay requirement (Table I):

$$x_{on}d_{p_{n0}} \leq d_o^{\max}, \quad \forall o, \forall n \in \mathcal{N}. \quad (6)$$

A. Objective Function

We aim to minimize the total network cost consisting of the computational cost and routing cost⁴. The computational cost of DU- n is:

$$V_n(\mathbf{x}_n) = \alpha_n + \beta_n \lambda_n \sum_{o=0}^3 \rho_o^d x_{on}. \quad (7)$$

We also have a computing cost for CU:

$$V_0(\mathbf{x}) = \sum_{n \in \mathcal{N}} \sum_{o=0}^3 x_{on} (\alpha_0 + \lambda_n \beta_0 \rho_o^c). \quad (8)$$

Then, the cost to route data flows from DU- n to CU is:

$$U_{n0}(\mathbf{x}_n) = \zeta_{p_{n0}} r_n(\mathbf{x}) \quad (9)$$

Finally, we have the total vRAN cost as:

$$J(\mathbf{x}) = \sum_{n \in \mathcal{N}} \left(V_n(\mathbf{x}_n) + U_{n0}(\mathbf{x}_n) \right) + V_0(\mathbf{x}), \quad (10)$$

which leads to the following problem:

$$\begin{aligned} \mathbb{P} : & \text{ minimize } J(\mathbf{x}) \\ & \text{ s.t } (2) - (6) \end{aligned}$$

\mathbb{P} is a combinatorial problem to decide the function placement \mathbf{x} for all BSs that having DU-CU path p_{n0} for each BS- n in network graph $G = (\mathcal{I}, \mathcal{E})$ with traffic load λ . Next, we discuss the complexity of \mathbb{P} .

⁴In this case, we follow the linear objective cost function similar to the previous studies [10], [11]. However, our solution approach does not restrict only to the linear objective. Our approach complies with the feedbacks from the penalty and reward signal; hence, it also can be tailored to a non-linear objective.

B. Complexity Analysis

The complexity of \mathbb{P} can be identified from the polynomial reduction of *multiple-choice multidimensional knapsack problem (MMKP)*.

MMKP. Let suppose there are N items with values v_1, v_2, \dots, v_N . We also have r_1, r_2, \dots, r_N correspond to the required resource to pick the items. In the 0-1 knapsack problem (KP), the aim is to pick the items $x_i \in \{0, 1\}$ that maximize the total values $\sum_{i=1}^N x_i v_i$, subject to constraint $\sum_{i=1}^N r_i \leq R$. This is a well-known NP hard problem and there is a pseudo-polynomial algorithm using a dynamic programming concept that has complexity $\mathcal{O}(NR)$ [34]. MKKP is a variant of 0-1 KP where there are M groups of items, e.g., group i has l_i items. Each item has a specific value v_{ij} correspond to j -th item of i -th group and needs K resources. Hence, each item in a group has a resource vector $\mathbf{r}_{ij} = (r_{ij1}, \dots, r_{ijK})$ and $\mathbf{R} = (R_1, \dots, R_K)$ is the resource bound of the knapsack. The aim is to exactly pick one item from each group, e.g., $\sum_{j=1}^{l_i} x_{ij} = 1, x_{ij} \in \{0, 1\}$ that maximize the total values: $\sum_{i=1}^M \sum_{j=1}^{l_i} x_{ij} v_{ij}$, subject to the resource constraint: $\sum_{i=1}^M \sum_{j=1}^{l_i} x_{ij} r_{ijk} \leq R_k, k = 1, \dots, K$.

Finding an exact solution for MMKP is also NP-hard [34]. It is also worth noting that the search space for solution in MMKP is smaller than other KP variants; hence, exact solution is not implementable in many practical problems as there is more limitation of picking items from a group in MMKP instance [34]. Next, We prove that \mathbb{P} is harder than MMKP.

Theorem 1. *MMKP can be reduced to \mathbb{P} in polynomial time, e.g., $\text{MMKP} \leq_P \mathbb{P}$.*

Proof. Let suppose we have unlimited link capacity, no routing cost and no the delay requirements. Hence, all path of DU-CU pair are eligible and (4)-(6) are always satisfied. This problem then can be mapped to MMKP by setting: 1) M groups to N BSs, 2) each i -th group with l_i items to BS- n with $|o| = 4$ of split options, 3) j -th item of i -th group to split configuration o_n of BS- n , 4) r_{ij} to the incurred computing load, e.g., $\lambda_n \rho_i^c$ and $\lambda_n \rho_i^d$, and 5) the knapsack constraints to computing constraints H_n and H_0 . The value v_{ij} of item- j in group- i also can be mapped with the costs (e.g., computing and routing) of deploying split- o of BS- n , where the MMKP is maximization problem and \mathbb{P} is a minimization problem. We can see the reduction is of polynomial time: we select the function split configuration for every BS correspond to that we activate an item that we pick to a knapsack in each group. Therefore, we can conclude that if we can solve \mathbb{P} in polynomial time we also can solve any MMKP problem.

IV. CONSTRAINED DEEP REINFORCEMENT BASED FUNCTIONAL SPLIT OPTIMIZATION

In supervised learning, the performance of the model depends on the quality of the supervised labels, where finding high-quality labelled data (e.g., optimal label) is expensive and may not be possible. Therefore, we follow NCO framework with deep RL paradigm [16], [17], [24]. We define *environment* as a vRAN system consisting of CU, DUs and network links. The *states* is defined as a sequence of all BS functions. Our RL *agent* generates *action* that corresponds to a set of decisions to choose the functional split configuration for every BS. This action decides which functions are deployed at the DU and CU for every BS. The environment will evaluate for every action taken and give a feedback signal from the environment. This feedback consists of *reward* (the total network cost) and *penalization* (constraint violation). As opposed to supervised learning, RL can deliver an appropriate paradigm for training and updating the neural network parameters to improve the performance of the model for the functional split problem. It simply relies on the reward and penalty feedbacks (interaction with the environment) instead of the high-quality labelled data. Since our problem is combinatorial that has highly dimensional action space, we leverage model-free policy-based RL that optimizes the weight parameter θ that infers a policy strategy to deploy the split configuration. It is worth noting that we have a constrained environment; hence, we also consider a constraint relaxation technique in the cost function of our policy-based method to deal with constraint dissatisfaction.

Our approach follows the deep RL paradigm based on the constrained policy optimization and neural network architecture to solve the functional split problem in the vRAN. We utilize Policy Gradient [27] with Lagrangian relaxation method [28]. In addition to the reward (cost) signal, we also give penalization for every constraint violation that guides the policy to constraint satisfaction. In this sense, the penalty coefficient (Lagrangian multiplier) setting is a multi-objective problem where there is a different optimum solution for each configuration. To this end, we follow two penalty coefficient updates: 1) CDRS-Fixed that uses a fixed penalty coefficient (reward shaping) [24], [35] and 2) CDRS-Ada that applies an adaptive penalty coefficient (updated in the ascent direction) [29]. A neural network architecture formed by an encoder-decoder sequence-to-sequence model [30], [31] based on stacked LSTM is also utilized that approximate the stochastic policy over the solution.

Our agent receives input of set of BS functions $\mathcal{F} = \{\mathcal{F}_n\}_{n=1}^N$ where $\mathcal{F}_n = \{f_0, f_1, f_2, f_3\}$ is a set of functions for BS- n . In the output, we expect to receive $\mathcal{O} = \{o_n\}_{n=1}^N$ as a set of selected configuration for all BSs. It addresses the split configuration of BS- n with $o_n \in \{0, 1, 2, 3\}$.

To this end, we use the neural network with weight parameter θ that infers a policy strategy $\pi_\theta(\mathcal{O}|\mathcal{F}, \theta)$ to deploy the split configuration. In practice, our approach does not have to know the defined problem in Section III. Our agent interacts with the environment expecting to receive a reward (network cost) and penalization (constraints violation); then learn from this interaction to find the optimal solution. At the test time, we perform an inference process through search strategies by a greedy decoding or temperature sampling method.

A. Neural Network Architecture

Our system is bounded under computational and link capacity, where each BS has distinct network parameters. Hence, the BS input sequence (to which BS needs to decide first) affects the solution. To this end, we use a sequence-to-sequence model with an attention mechanism, formed by encoder-decoder design and based on stacked LSTM cell [30], [31]. We also draw a batch of B i.i.d samples with different sequence order when training our model. Additionally, the attention gives information on how strongly the element of a sequence is correlated to each other; hence it allows to capture the correlation of BSs characteristic.

Our neural network infers a solution policy strategy to deploy the function split configuration for all BS, given a sequence of BSs as an input $\mathcal{F} = \{\mathcal{F}_1, \dots, \mathcal{F}_N\}$. The encoder read the entire input sequence to a fixed-length vector. Then, the decoder decides the functional split configuration of a BS at each step from an output function based on its own previous state combined with an attention over the encoder hidden states [31]. The decoder network hidden state is defined with a function: $\mathbf{h}_t = f(\mathbf{h}_{t-1}, \bar{\mathbf{h}}_{t-1}, \mathbf{c}_t)$. Our model also needs to derive a context vector \mathbf{c}_t that captures relevant source information at each step t that help predicting the current deployed split configuration. The main idea is to use attention where the context vector \mathbf{c}_t takes consideration of all the hidden states of the encoder and the alignment vector \mathbf{a}_t as:

$$\mathbf{c}_t = \sum_{k \in \mathcal{F}} \mathbf{a}_{tk} \bar{\mathbf{h}}_k. \quad (11)$$

Note that the alignment vector has an equal size to the number of step on the source side. It can be calculated by comparing the current target hidden state of decoder \mathbf{h}_t with each source hidden state $\bar{\mathbf{h}}_k$, hence:

$$\mathbf{a}_{tk} = \frac{\exp(\text{score}(\mathbf{h}_t, \bar{\mathbf{h}}_k))}{\sum_{k'=1}^N \exp(\text{score}(\mathbf{h}_t, \bar{\mathbf{h}}_{k'}))} \quad (12)$$

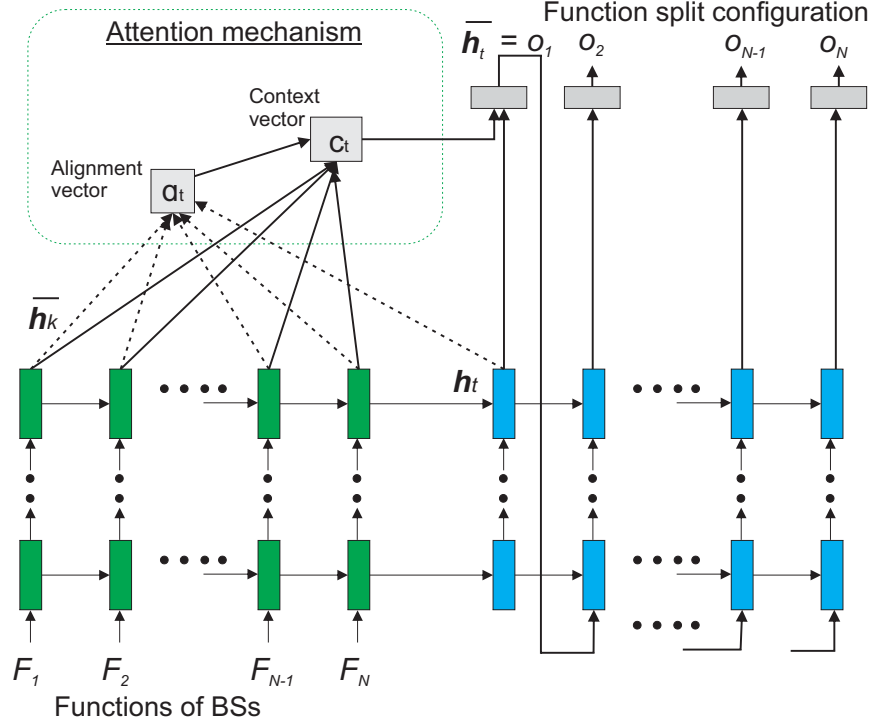


Fig. 2: **Neural network architecture.** It is formed by an encoder-decoder sequence-to-sequence model based on stacked LSTM networks.

This alignment model gives a score a_{tk} which describes on how well the pair of input at position k and the output at position t . The alignment score is parametrized by a feed-foward network where the network is trained jointly with the other models [31]. Hence, the score function is defined by non-linear activation function following Bahdanau's additive style:

$$\text{score}(\mathbf{h}_t, \bar{\mathbf{h}}_k) = \mathbf{v}_a^\top (\tanh(\mathbf{w}_1 \mathbf{h}_t + \mathbf{w}_2 \bar{\mathbf{h}}_k)), \quad (13)$$

where $\mathbf{v}_a^\top \in \mathbb{R}^n$, $\mathbf{w}_1 \in \mathbb{R}^{n \times n}$ and $\mathbf{w}_2 \in \mathbb{R}^{n \times 2n}$ are the weight matrices to be learned in the alignment model, and n is the number of neural network layers. The overall architecture is depicted in Fig 2.

B. Constrained Policy Gradient with Baseline

A Policy gradient method is applied to learn the parameters of the stochastic policy $\pi_\theta(\mathcal{O}|\mathcal{F}, \theta)$. It predicts the split configuration that minimizes the total cost by assigning a high probability to o_n for having a lower cost and a low probability for a higher cost. Our neural network uses the chain rule for factorizing the output probability:

$$\pi_\theta(\mathcal{O}|\mathcal{F}, \theta) = \prod_{n=1}^N \pi_\theta(o_n|o_{(<n)}, \mathcal{F}_n). \quad (14)$$

We define the objective of \mathbb{P} as an expected reward that is obtained for every vector of weight θ . Hence, the expected cost J is associated with the selected configuration given BS- n functions:

$$J^\pi(\theta|\mathcal{F}_n) = \mathbb{E}_{o_n \sim \pi(\cdot|\mathcal{F}_n)}[J(o_n)], \quad (15)$$

and we have the expected of total cost of all BS:

$$J^\pi(\theta) = \mathbb{E}_{o_n \sim \mathcal{O}}[J(\theta|\mathcal{O})]. \quad (16)$$

Our system model has constraints of delay requirements, computational, and link capacities. Hence, we define $J_C^\pi(\theta) = (J_{C_i}^\pi(\theta), \forall i)$ as a function of constraint dissatisfaction to capture the penalization that the environment returns for violating each i constraint requirement, e.g., computing, link, delay. Our original problem turns to a primal problem:

$$\mathbb{P}_{1P} : \min_{\pi \sim \Pi} J^\pi(\theta); \quad \text{s.t. } J_C^\pi(\theta) \leq 0.$$

In this problem, we consider parametrized policies using neural network. In order to ensure the convergence of our policy to a constraint satisfaction, we follow [36] and make the assumptions:

Assumption 1. J^π is bounded for all policies $\pi \in \Pi$.

Assumption 2. Each local minima of $J_C^\pi(\theta)$ is a feasible solution.

Assumption 2 describes that any local minima π_θ satisfies all constraints, e.g., $J_C^\pi(\theta) \leq 0$. It is the minimal requirement that guarantees the convergence of a gradient algorithm to a feasible solution. The stricter assumption, e.g., convexity, may guarantee the optimal solution.

Next, we reformulate \mathbb{P}_{1P} to unconstrained problem with Lagrange relaxation [28]. The penalty signal is also included aside of original objective for infeasibility, which leads to a sub-optimality for infeasible solutions. Given \mathbb{P}_{1P} , we have the dual function:

$$\begin{aligned} g(\mu) &= \min_{\theta} J_L^\pi(\mu, \theta) = \min_{\theta} J^\pi(\theta) + \sum_i \mu_i J_{C_i}^\pi(\theta) \\ &= \min_{\theta} J^\pi(\theta) + J_\zeta^\pi(\xi), \end{aligned} \quad (17)$$

where $\mu = (\mu_i, \forall i)$, $J_L^\pi(\mu, \theta)$ and $J_C^\pi(\xi)$ are the penalty coefficient (Lagrange multiplier), Lagrange objective function and the expected penalization, respectively. Then, we define the dual problem:

$$\mathbb{P}_{1D} : \max_{\mu} g(\mu).$$

\mathbb{P}_{1D} aims to find a local optima or a saddle point $(\theta(\mu^*), \mu^*)$, which is a feasible solution. The feasible solution is a solution that satisfies: $J_{C_i}^\pi(\theta) \leq 0, \forall i$. To compute the weight parameter θ that optimizes the objective, we utilize Monte-Carlo Policy Gradient and stochastic gradient descent:

$$\theta_{k+1} = \theta_k - \eta_a(k) \nabla_{\theta} J_L^\pi(\mu, \theta), \quad (18)$$

where $\eta_a(k)$ is the step-size (agent). The gradient $\nabla_{\theta} J_L^\pi(\mu, \theta)$ can be calculated with log-likelihood method as:

$$\nabla_{\theta} J_L^\pi(\theta) = \mathbb{E}_{\mathcal{O} \sim \pi_{\theta}(\cdot|\mathcal{F})} [L(\mathcal{O}|\mathcal{F}) \nabla_{\theta} \log \pi_{\theta}(\mathcal{O}|\mathcal{F})], \quad (19)$$

and $\nabla_{\mu} J_L^\pi(\mu, \theta) = \mathbb{E}_{\mathcal{O} \sim \pi_{\theta}(\cdot|\mathcal{F})} [C(\mathcal{O}|\mathcal{F})]$. The total cost with penalization, $L(\mathcal{O}|\mathcal{F})$, consists of the total network cost and the weighted sum of penalization: $L(\mathcal{O}|\mathcal{F}) = J(\mathcal{O}|\mathcal{F}) + \xi(\mathcal{O}|\mathcal{F})$, where $J(\mathcal{O}|\mathcal{F})$ is the total operating cost in each iteration and $\xi(\mathcal{O}|\mathcal{F}) = \mu C(\mathcal{O}|\mathcal{F})$ is the weighted sum of constraint dissatisfaction of $C(\mathcal{O}|\mathcal{F})$.

The penalty coefficient μ is set manually [24], [35] for CDRS-Fixed within a range $[0, \mu_{\max}]$ ⁵. In this case, the selection of μ can be set following intuition approach in [24] (Appendix C), i.e., agent will not pay attention to penalty if $\mu = 0$, and it will only converge to penalization if $\mu = \infty$. Hence, selecting appropriate penalty coefficient is important in this case. Otherwise, we can follow a less intuitive approach by adaptively updating the penalty coefficient (CDRS-Ada). CDRS-Ada is updated based on primal-dual optimization (PDO) method inspired from [29]. Hence, we update the penalty coefficient in the ascent direction as:

$$\mu_{k+1} = \mu_k + \eta_d(k) \nabla_{\mu} J_L^\pi(\mu, \theta) \quad (20)$$

$$= \mu_k + \eta_d(k) (J_C^\pi(\theta))_+, \quad (21)$$

where $\eta_d(k)$ is the step-size (Dual). The penalty coefficient μ_k is updated for every k -th iteration

⁵If Assumption 2 is satisfied, μ_{\max} can be set to ∞ [36].

and will converge to a fixed value once the constraints are satisfied [29], [36]. Next, we use Monte-Carlo sampling to approximate the gradient by drawing B i.i.d samples $\mathcal{F}^1, \dots, \mathcal{F}^B \sim \mathcal{F}$; hence, the gradient can be written as:

$$\nabla_{\theta} J_L^{\pi}(\theta) \approx \frac{1}{B} \sum_{i=1}^B \left(L(\mathcal{O}^i | \mathcal{F}^i) - b_{\theta_v}(\mathcal{F}^i) \right) \nabla_{\theta} \log \pi_{\theta}(\mathcal{O}^i | \mathcal{F}^i). \quad (22)$$

Baseline estimator. The baseline choice can be from an exponential moving average of the reward over the time that captures the improving policy in training. Although it succeeds in the Christofides algorithm, it does not perform well because it can not differentiate between different input [16]. To this end, we use a parametric baseline b_{θ_v} to estimate the expected total cost with penalization $\mathbb{E}_{\mathcal{O} \sim \pi(\cdot | \mathcal{F})} L(\mathcal{O} | \mathcal{F})$ that typically improves learning performance. We train the baseline in an auxiliary network built from an LSTM encoder connected to a multilayer perceptron output layer similar to [24]. The auxiliary network (parameterized by θ_v) that learns the expected cost with penalization by the current policy π_{θ} from given input \mathcal{F} , is trained with stochastic gradient descent. It employs a mean squared error (MSE) objective, calculated from its prediction b_{θ_v} and the actual cost with penalization, and sampled by the most recent policy (obtained from the environment). We formulate the auxiliary objective:

$$\mathcal{L}(\theta_v) = \frac{1}{B} \sum_{i=1}^B \|b_{\theta_v}(\mathcal{F}^i) - L(\mathcal{O}^i | \mathcal{F}^i)\|_2^2. \quad (23)$$

Algorithm 1 summarizes our training algorithm based on a single time-step Monte-Carlo Policy Gradient with a baseline estimator, which runs until K epochs. The sequence of policy updates will converge to a locally optimal policy, and the penalty coefficient updates (CDRS-Ada) will converge to a fixed value when all constraints are satisfied; see also [29], [36].

C. Searching Strategy

At the test time, evaluating the total network cost is inexpensive. Our agent can add a search procedure during the inference process by considering solution candidates from multiple trained models and select the best. This can help to reduce the inferred policy suffering from a severe suboptimality. In this part, we employ two different search strategies: a greedy decoding and sampling method with temperature hyperparameter [16].

Greedy decoding. It is the simplest search strategy. The idea is to select the function split configuration with the largest probability for having the lowest cost at each decoding step. It learns over multiple trained models. Then, at inference time, the greedy output from each model

Algorithm 1: CDRS Training

Input: K (Num of epoch), B (Batch size), \mathcal{F} (Learning set)

Initialize: assign agent and critic (baseline) networks with random weights θ and θ_v .

```
1 for  $k = 1, \dots, K$  do
2    $d\theta \leftarrow 0$  % Reset gradient
3    $\mathcal{F}^i \sim \text{SampleInput}(\mathcal{F})$  for  $i \in \{1, \dots, B\}$ .
4    $\mathcal{O}^i \sim \text{SampleSolution}(\pi_\theta(\cdot|\mathcal{F}))$  for  $i \in \{1, \dots, B\}$ .
5    $b^i \leftarrow b_{\theta_v}(\mathcal{F}^i)$  for  $i \in \{1, \dots, B\}$ .
6   Compute  $L(\mathcal{O}^i)$  for  $i \in \{1, \dots, B\}$ .
7    $g_\theta \leftarrow \frac{1}{B} \sum_{i=1}^B (L(\mathcal{O}^i) - b^i) \nabla_{\theta} \log \pi_{\theta}(\mathcal{O}^i|\mathcal{F}^i)$  from (22).
8    $\mathcal{L}_v \leftarrow \frac{1}{B} \sum_{i=1}^B \|b^i - L(\mathcal{O}^i)\|_2^2$  from (23).
9    $\theta \leftarrow \text{Adam}(\theta, g_\theta)$  %Run Adam algorithm
10   $\theta_v \leftarrow \text{Adam}(\theta_v, \mathcal{L}_v)$  %Run Adam algorithm
11  Update  $\mu$  from (20) %CDRS-Ada
12  Set  $\mu = \max(0, \mu)$  %CDRS-Ada
13 end
14 return  $\theta, \theta_v, \mu$ 
```

is evaluated to find the best one [24]. Hence, we can extend our CDRS framework to CDRS-Fixed-G that uses a fixed penalty coefficient with greedy decoding for the inference process and CDRS-Ada-G that uses an adaptive penalty coefficient with greedy decoding.

Temperature sampling. This method samples multiple candidate solutions from stochastic policy for every trained model, then select the split configuration with the lowest total cost [16], [24]. As opposed to the heuristic solvers, it does not sample the different split options during the process. Instead, it allows to control the sparsity of the output distribution with a temperature hyperparameter T . Hence, the softmax function in (12) is modified, e.g., to $\mathbf{a}_{tk} = \frac{\exp(\text{score}(\mathbf{h}_t, \bar{\mathbf{h}}_k)/T)}{\sum_{k'=1}^N \exp(\text{score}(\mathbf{h}_t, \bar{\mathbf{h}}_{k'})/T)}$ (softmax temperature). In this case, the temperature hyperparameter T during the training process is equal to 1. In the test, we set $T > 1$, hence the output distribution becomes less step and prevents the model from being overconfident. With this method, we can extend the CDRS framework to CDRS-Fixed-T (fixed penalty coefficient, temperature sampling) and a CDRS-Ada-T (adaptive penalty coefficient, temperature sampling)

V. RESULTS AND DISCUSSION

In this section, we conduct several experiments to evaluate our approach using synthetic and real network datasets. We aim to examine our approach in regards to: (i) the behaviour during the training process, (ii) the accuracy and solution distributions to the optimality with different

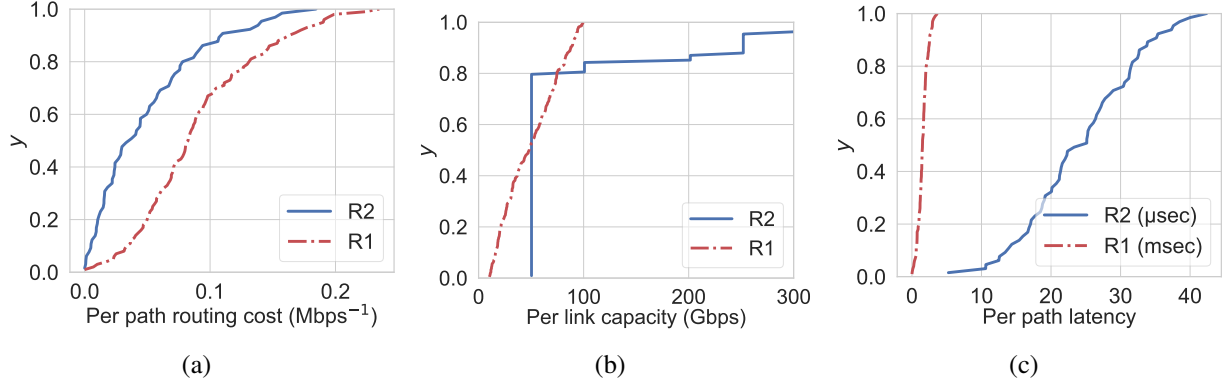


Fig. 3: **RANs dist.** eCDF of (a) per-path routing cost, (b) per-link capacity, (c) per-path latency for R1 and R2.

penalty coefficient settings and search strategies, (iii) the impact of routing costs and traffic loads on the optimality performance and total network cost, and (iv) the computational time.

A. Environment & Experiment Setup

We use synthetic (R1) and real (R2) network datasets to evaluate our approach. R1 is generated using Waxman algorithm [32] with parameters such as link probability (α) and edge length control (β). These respective parameters (α, β) are set to (0.5, 0.1). R1 has 100 nodes consisting of 1 CU and 99 DUs. In the case of R2, we utilize a real network dataset from [37]. R2 has 64 nodes with 1 CU and 63 DUs. R1 and R2 differ in parameters, e.g., location, link capacity, weighted link, delay. We use a standard store-and-forward model to calculate the delay. It is from $12000/c_{ij}$, $4\mu\text{secs/Km}$ and $5\mu\text{secs}$ for transmission, propagation and processing delay, respectively; see [11]. The link capacity varies to 100 Gbps (R1) and 252 Gbps (R2). The path delay reaches to $3658 \mu\text{s}$ (R1) and $42 \mu\text{s}$ (R2). In R1, the routing cost per path depends on the cost per selected link where it comes from randomly generated for each link. A link with a routing cost of 1 monetary unit per Mbps means having the same cost as a DU computing cost. We consider the routing cost within a range of $0.001 - 0.01$ times of DU computing cost (for the same network load) for each link in R1. In R2, we calculate the distance between nodes based on its geolocation dataset from [37] and charge the cost of 0.01 monetary unit per Mbps/km. We generate R1 that has stricter constraints and a larger scale environment than R2. Fig. 3 depicts the parameter distributions of our RANs with eCDF.

In this experiment, all system parameters correspond to testbed measurements of previous studies [7], [10]–[12], [38]. We assume a high load scenario $\lambda_n = 150$ Mbps for every DU. This

setting is based on 1 user/TTI, 2×2 MIMO, 20 Mhz (100 PRB), 2 TBs of 75376 bits/subframe and IP MTU 1500B. We use an Intel Haswell i7-4770 3.40GHz CPU as the *reference core*, and set the maximum computing capacity to 75 RCs for CU and 7.5 RCs for each DU. Each split configuration $o \in \{0, 1, 2, 3\}$ incurs computational load $\rho_o^d = \{0.05, 0.04, 0.00325, 0\}$ RCs per Mbps for DU and $\rho_o^c = \{0, 0.001, 0.00175, 0.05\}$ RCs per Mbps for CU, respectively. The VM instantiation cost of CU is a half of DU ($\alpha_0 = \alpha_n/2$) and the processing cost is set to $\beta_0 = 0.017\beta_n$.

Our learning rate is initially set to $\eta_a = 0.0001$ (Agent) and $\eta_b = 0.005$ (Baseline) with the batch size: 128. Our neural network has the number of layers, hidden dimension and embedding size with 1, 32 and 32, respectively. The temperature hyperparameter is set to $T = 1$ by default, so the model computes the softmax function directly. We scale all the original values of weighted paths and traffic loads randomly with uniform distribution $[0, 1]$ as in [16]. Then, we generate three models (RL-pretaining) as an output of our training with 50000 (in R1) and 15000 (in R2) epochs each. CDRS-Fixed uses a fixed penalty coefficient with $\mu_i = 1, \forall i$ for all epochs while CDRS-Ada is set with initial penalty coefficient $\mu_i(0) = 1, \forall i$ and step-size $\eta_d = 0.001$. The training is performed with Tensorflow 1.15.3 and Python 3.7.4. In the test, the temperature sampling method uses 16 samples and $T = 15$ (softmax temperature).

B. Training Analysis

We aim to examine the behaviour of CDRS-Fixed and CDRS-Ada during the training process in R1 and R2. We focus on the mini-batch loss, reward (total network cost), Lagrangian cost and penalization.

Fig. 4 visualizes the training of CDRS-Fixed and CDRS-Ada in R1 and R2. We found additional cost because of penalization at the beginning of the training for both settings in R1 and R2. It occurs because CDRS-Fixed and CDRS-Ada try to find the solution, but it violates the constraint sets (e.g., latency, bandwidth, computation); hence, it receives additional cost penalization. It also shows a significant difference in the cost of penalization in R1 compared to R2. The main reason is that R1 has stricter constraints, e.g., larger path delays, smaller link capacity than R2. We can also see that CDRS-Fixed and CDRS-Ada improve their policy by focusing on constraint satisfaction and then correcting the weights via stochastic gradient descent. It is proven from our agents' behaviour where the penalization value keeps decreasing and turns to zero as soon as the training goes. CDRS-Ada also sets the penalty coefficient increasing in the

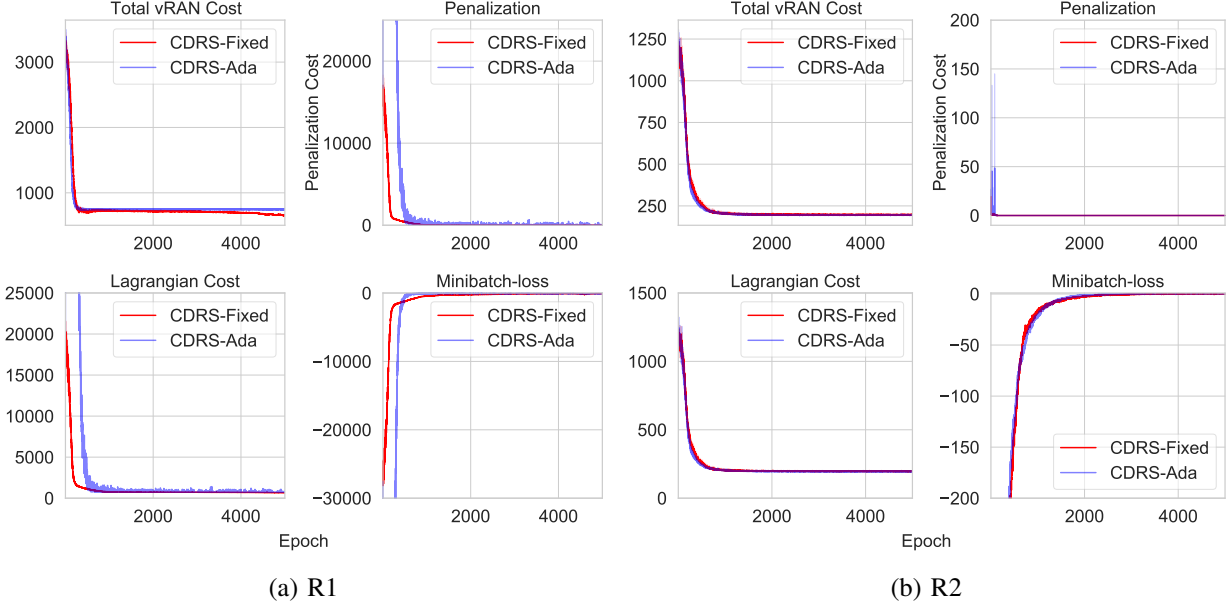


Fig. 4: **Training results of CDRS in (a) R1 and (b) R2.** CDRS-Fixed uses a fixed value of penalty coefficient (reward shaping) with $\mu_i = 1, \forall i$. CDRS-Ada utilizes an adaptive update of penalty coefficient.

ascent direction that causes a higher penalization value than CDRS-Fixed. However, it can help to speed up (CDRS-Ada penalization downs faster than CDRS-Fixed) the policy to constraint satisfaction where the penalization value turns to zero.

We also found that the policy of CDRS-Ada converges faster than CDRS-Fixed from the behaviour of mini-batch loss in R1. Despite the mini-batch loss decreasing to near zero after several epochs as both settings improve their policy, the mini-batch loss of CDRS-Ada diminishes faster to near zero than CDRS-Fixed. However, CDRS-Ada suffers from more severe suboptimality. It is shown by the total vRAN cost of CDRS-Ada that converges to a fixed value but having a higher cost compared to CDRS-Fixed. Then, we have the Lagrangian cost that considers both vRAN and penalization cost. It describes how our agent tries to minimize the primal problem \mathbb{P}_{IP} through the dual problem \mathbb{P}_{ID} . When our agent finally dismisses the penalization cost, it means that all constraints are satisfied. As a result, the Lagrangian cost becomes equal to the vRAN cost, and the penalty coefficient of CDRS-Ada converges to a fixed value. Although having different behaviours, CDRS-Ada and CDRS-Fixed can learn the solution and converge to the local minima or saddle point in R1 and R2.

Findings: 1) R1 has stricter constraint requirements than R2; hence, it gives higher additional cost for penalization to CDRS-Fixed and CDRS-Ada. 2) CDRS-Fixed and CDRS-Ada improve

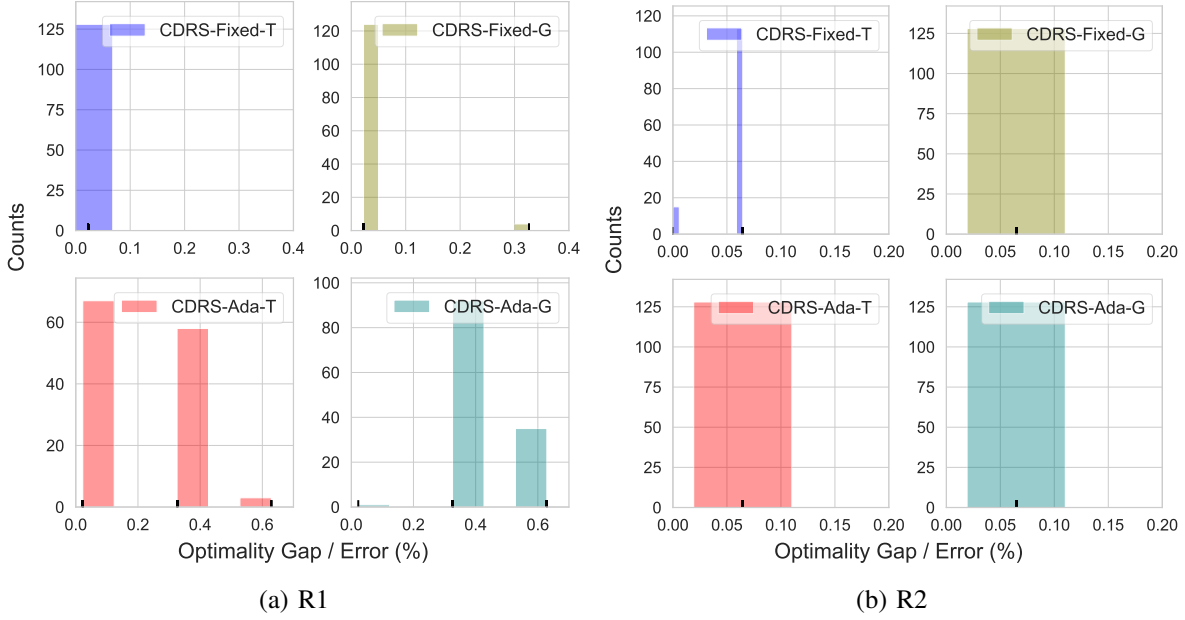


Fig. 5: **Histogram of CDRS accuracy in (a) R1 and (b) R2.** The accuracy is calculated over 128 test. CDRS-Ada-T and CDRS-Fixed-T are set with $T = 15$ and 16 samples.

their policy by focusing on the penalization; then, it adjusts its weight as the training goes. 3) CDRS-Ada receives higher penalization compared to CDRS-Fixed as a result of increasing the penalty coefficient in the ascent direction; however, it also helps to speed up the policy to constraint satisfaction. 4) CDRS-Ada converges faster but has a higher cost than CDRS-Fixed in R1. 5) When all constraints are satisfied, the Lagrangian cost becomes equal to the total vRAN cost and the penalty coefficient of CDRS-Ada converges to a fixed value.

C. Accuracy of Solutions

In this part, we study the accuracy of CDRS over different penalty coefficient settings and search strategies: CDRS-Fixed-G, CDRS-Fixed-T, CDRS-Ada-G and CDRS-Ada-T. We conduct 128 tests (with distinct sequence order of BSs) in R1 and R2 to assess how accurate these four CDRS settings find the solution of the vRAN split problem. We utilize three RL-Pretrained models as a result of our CDRS training.

Fig. 5 shows the distribution of the solutions of CDRS-Fixed-G, CDRS-Fixed-T, CDRS-Ada-G and CDRS-Ada-T in R1 and R2. It is clearly shown that all of these settings can guarantee less than 0.6% (R1) and 0.1% (R2) of the optimality gap. In a stricter environment (R1), CDRS-Fixed-G and CDRS-Fixed-T perform better by offering lower solution errors ($\leq 0.05\%$ and $\leq 0.05\%$ of optimality gap) than CDRS-Ada-G and CDRS-Ada-T ($\leq 0.6\%$). It means that a fixed penalty

coefficient setting can lead to a better optimality performance during the test than the adaptive one. However, CDRS-Fixed-G, CDRS-Ada-G and CDRS-Ada-T have a similar performance in R2. Regardless of R1 or R2, using a sampling method with a temperature hyperparameter can improve (or at least at same) the optimality performance than Greedy decoding. It is shown from the higher total number of solutions (counts) for a sampling method that having a lower error. The combination of a fixed penalty in the training and temperature sampling method (CDRS-Fixed-T) can improve the solution performance significantly both in R1 and R2. It can achieve an optimal value (R2) and less than 0.05% of error for a more complex environment (R1). It is also shown that CDRS-Fixed-T is less affected to the stricter environment than any other settings where all of the distribution solutions are in less than 0.05%.

Findings: 1) CDRS-Fixed-G, CDRS-Fixed-T, CDRS-Ada-G and CDRS-Ada-T can guarantee the solution with very close to the optimal value offering less than 0.6% (R1) and 0.1% (R2) of the optimality gap over 128 tests. 2) CDRS-Fixed-T can significantly improve the optimality performance (offers $\leq 0.05\%$ of optimality gap) and outperforms the other settings.

D. Impact of Routing Cost

This part studies the impact of altering the routing cost to CDRS-Fixed-G, CDRS-Fixed-T, CDRS-Ada-G and CDRS-Ada-T. We aim to examine how the routing cost affects optimality performance and the total network cost. Hence, the default routing cost is changed within a range of $\gamma = 0.1$ to $\gamma = 1$. This change can arise due to increasing or decreasing the leasing agreement's price, maintenance, etc. The traffic load is fixed with $\lambda_n = 150$ Mbps. We utilize three our RL pretrained model, conduct 128 tests for each routing cost scale and analyze the offered solutions' distribution. We also consider benchmarking with two extremes of RAN setups, fully D-RAN and C-RAN⁶ to assess how significant the routing cost affects the total network cost over various RAN setups.

Fig. 6 depicts how the routing cost affects the optimality performance of CDRS-Fixed-G, CDRS-Fixed-T, CDRS-Ada-G and CDRS-Ada-T. It shows that the optimality gap (error) diminishes as the routing cost increases; then, it converges to a specific value. In R1, we see an improvement as the error decreases for CDRS-Fixed-G ($\approx 400\%$), CDRS-Fixed-T ($\approx 400\%$), CDRS-Ada-G ($\approx 450\%$) and CDRS-Ada-T ($\approx 400\%$). It also shows that CDRS-Ada-G gets

⁶We practically can not implement C-RAN because our RAN does not meet the constraint requirements of delay, bandwidth and CU capacity to deploy C-RAN. The presented C-RAN in this experiment is just for benchmarking; hence we also do not consider the penalization cost (constraints violation) for this case.

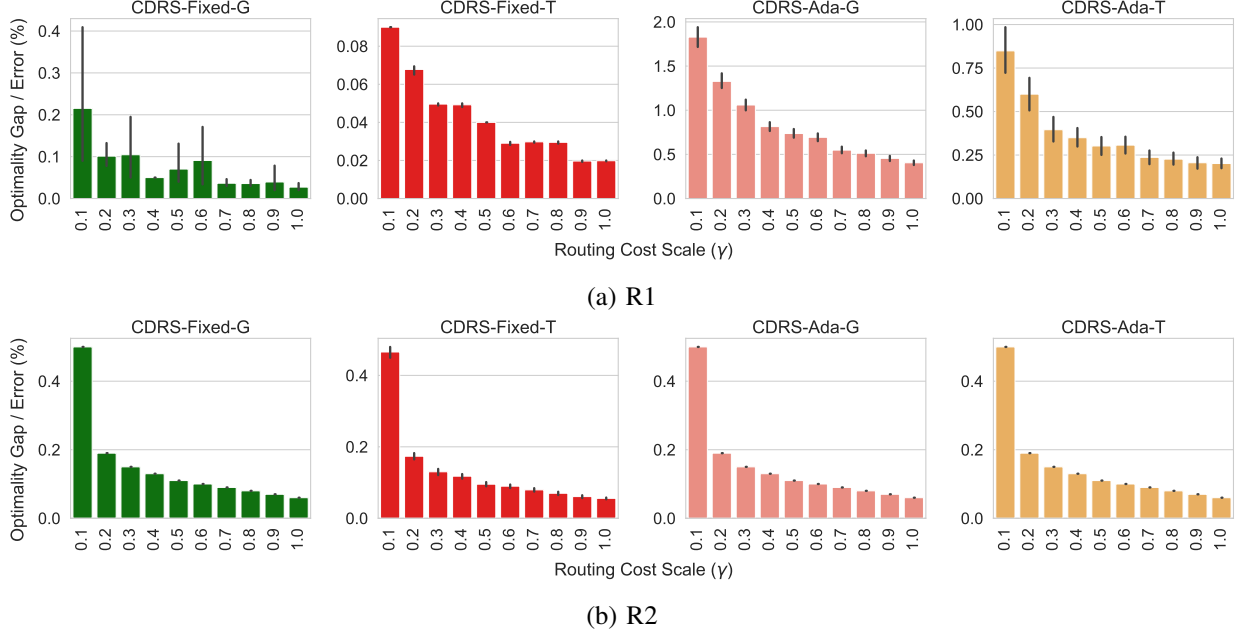


Fig. 6: **Impact of the routing cost to the accuracy in (a) R1 and (b) R2.** Study of altering the routing cost to the optimality performance with $\lambda_n = 150$ Mbps, $\forall n \in \mathcal{N}$. There are 128 tests for each routing scale $[0.1, 1]$.

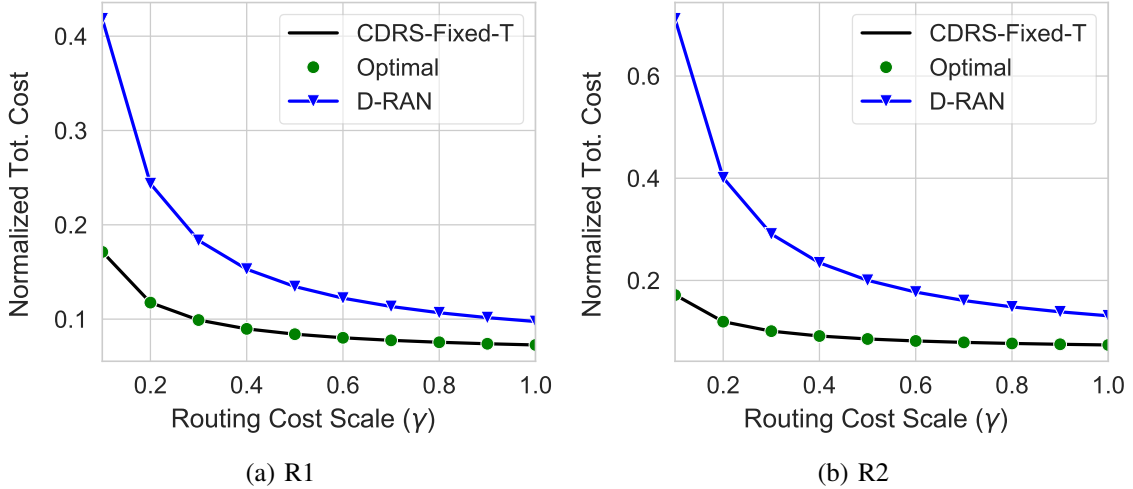


Fig. 7: **Impact of routing cost to the total cost in (a) R1 and (b) R2.** We also compare our approach (e.g., CDRS-Fixed-T) to two extreme cases: fully D-RAN and C-RAN, and the optimal value with the routing cost scaling from 0.1 to 1 of default R1 and R2. The presented cost above is normalized toward fully C-RAN cost.

the most impact while CDRS-Fixed-T is the least affected. However, all settings have a similar impact with ten-fold improvement in terms of error in R2. Although we have changed the routing cost from the default parameter, we found that routing cost gives relatively less effect to these settings where the error is maintained under 1.8% (CDRS-Ada-G at $\gamma = 0.1$). CDRS-Fixed-T

also remarkably can guarantee the solution under 0.08% ($\gamma = 0.1$).

Fig. 7 shows the routing cost's effect on the total network cost of CDRS-Fixed-T and D-RAN, normalized to the C-RAN cost in R1 and R2. It shows that the increase of routing cost gives CDRS-Fixed-T and D-RAN cost relatively decrease (around 320% and 420% from $\gamma = 0.1$ to $\gamma = 1$ in R1) to the C-RAN cost. Hence, we can conclude that the routing cost gives more impact to C-RAN than other setups. Additionally, CDRS-Fixed-T is the most cost-efficient with around 500% and 200% cost-saving of C-RAN and D-RAN at low routing cost ($\gamma = 0.1$). It also can save to 20 times and two-fold compared to the respective RAN setups at high routing cost ($\gamma = 1$) in R1. In R2, CDRS-Fixed-T can save to around five times and two times of C-RAN and D-RAN cost at low routing cost ($\gamma = 0.1$). It has cost-saving to 20 times and two-fold compared to the respective RAN setups at high routing cost ($\gamma = 1$). CDRS-Fixed-T offers the solution very close to the optimal solution ($\leq 0.09\%$ in R1 and $\leq 0.5\%$ in R2) and efficiently adapts to the change of the routing cost.

Findings: 1) The increase of routing cost lead to the reduction of the optimality gap; then, the reduction rate diminishes, and the optimal gap converges to a fixed value. 2) CDRS-Fixed-T is the least affected by the routing cost change, while CDRS-Ada-G is the most affected. 3) Altering the routing cost ($\gamma = [0.1, 1]$) does not significantly degrade the optimality performance. 4) The routing cost affects C-RAN setup at the most. 5) CDRS-Fixed-T has the lowest optimality gap, efficiently adapts to the change of the routing cost, and becomes the most cost-effective setup in R1 and R2.

E. Impact of Traffic Load

In this part, we assess how traffic load affects optimality performance and the total network cost. We change the traffic load from 10 Mbps to 150 Mbps. This evaluation is conducted using three pre-trained models and then examined with 128 tests.

Fig 8 shows the impact of altering the traffic load to the optimality performance of CDRS-Fixed-G, CDRS-Fixed-T, CDRS-Ada-G and CDRS-Ada-T. In R1, it shows that the increase of traffic load in line with the rise of the error to CDRS-Ada-G and CDRS-Ada-T, but it then diminishes to a fixed value, i.e., around 0.4% (CDRS-Ada-G) and 0.18% (CDRS-Ada-T). However, the traffic load does not significantly affect CDRS-Fixed-G and CDRS-Fixed-T, where they stay at around 0.04% and 0.02% of errors, respectively, in R1. In R2, CDRS-Fixed-G, CDRS-Fixed-T, CDRS-Ada-G and CDRS-Ada-T have the same trend where the optimality

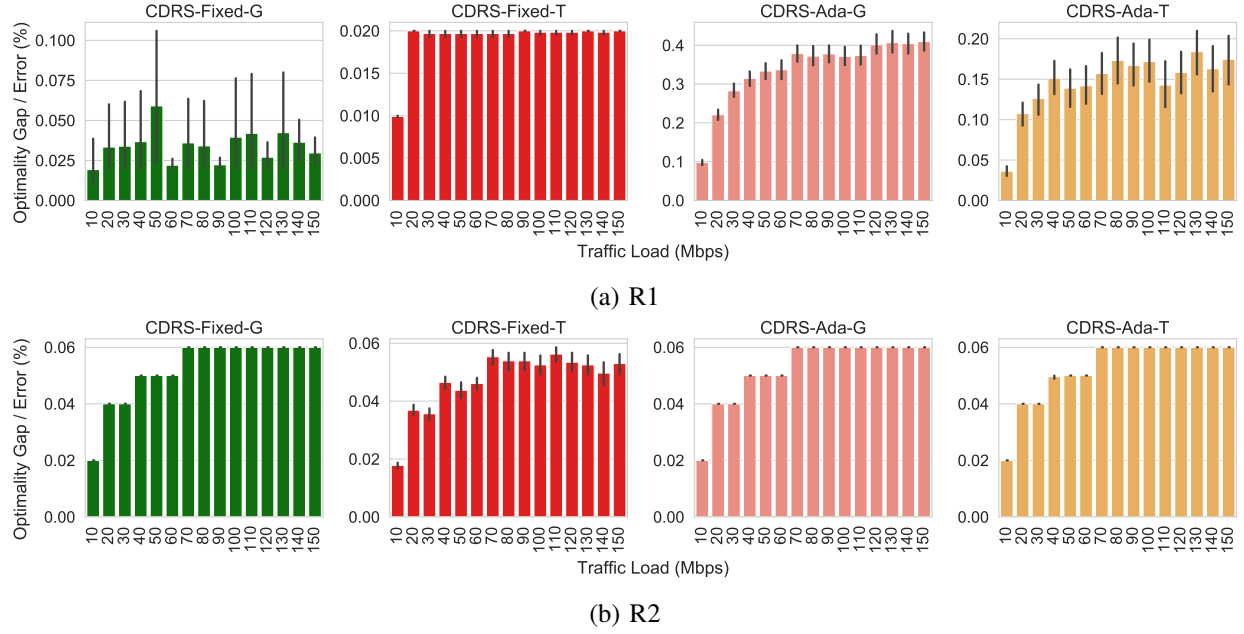


Fig. 8: **Impact of the traffic load to the accuracy in (a) R1 and (b) R2.** Study of traffic load to the optimality performance. There are 128 tests for each traffic load.

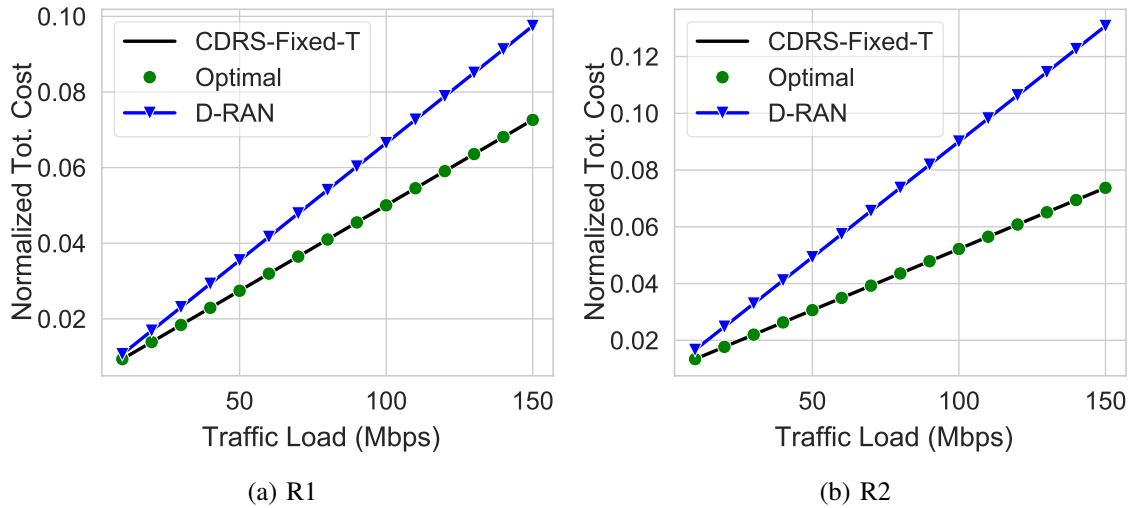


Fig. 9: **Impact of traffic load to total vRAN cost in (a) R1 and (b) R2.** On the comparison of our approach (e.g., CDRS-Fixed-T) to fully D-RAN. The presented cost above is normalized toward fully C-RAN cost.

gap increases with the traffic load; then, it diminishes at around 0.05%. We also found that CDRS-Fixed-T can lead to better optimality performance and a more stable solution.

Fig 9 examines the impact of traffic load to CDRS-Fixed-T and D-RAN cost normalized to the C-RAN cost. Despite an increase in CDRS-Fixed-T cost as the traffic load rise, it shows that CDRS-Fixed-T is still the most cost-effective compared to D-RAN and C-RAN R1 and R2.

Topology	MIP Solver	CDRS-Fixed-T	CDRS-Fixed-G	CDRS-Ada-T	CDRS-Ada-G
R1	0.2527	0.2026	0.0155	0.1985	0.0120
R2	0.1756	0.1240	0.0098	0.1207	0.0077

TABLE II: **Computational time.** Study of computational time for solving a single problem instance in seconds. The presented computational time is a result of averaging 128 executions.

In R1, CDRS-Fixed-T can save 114% at low traffic load (10 Mbps) and 134% at high traffic load (150 Mbps) of D-RAN cost, while 124% and 177% for the respective load in R2. The cost-saving gap is also more prominent with the increase of traffic load. We also found that D-RAN is the most affected by the increase in traffic load.

Findings: 1) CDRS-Fixed-T can offer to better optimality performance and more stable solution. 2) In R2, all CDRS settings have similar trends where the increase of traffic load can also increase the optimality gap, but it then diminishes and stays at around 0.05% for CDRS-Fixed-T and 0.06% for the others. 3) CDRS-Fixed-T is the most cost-efficient compared to C-RAN and D-RAN. 4) The increase of network cost in line with the traffic load where D-RAN is the most affected one.

F. Computational Time

Finally, we examine the computational time to solve a single instance of the vRAN split problem. We use a small laptop with an Intel Core i5-7300U CPU@2.60GHz and 8GB memory. The computational time for each CDRS setting is a result of averaging 128 executions with a trained model. We report this evaluation in Table II. Overall, our proposed CDRS settings: CDRS-Fixed-G, CDRS-Fixed-T, CDRS-Ada-G and CDRS-Ada-T have a faster computational time than MIP Solver. CDRS-Ada-G is the fastest with 0.0120 secs and 0.0077 secs in R1 and R2 reaching to 22.82 times faster than MIP Solver. We also found that any CDRS settings with a greedy decoding for the inference process, e.g., CDRS-Fixed-G, CDRS-Ada-G, is more time-efficient than a temperature sampling method with around 10-20 times faster. It is also shown that CDRS-Ada-G/T has a slightly faster computational time than CDRS-Fixed-G/T. Finally, we can sort from the fastest computational time as 1) CDRS-Ada-G, 2) CDRS-Fixed-G, 3) CDRS-Ada-T, 4) CDRS-Fixed-T, 5) MIP Solver.

Findings: 1) CDRS-Ada-G, CDRS-Fixed-G, CDRS-Ada-T, and CDRS-Fixed-T can reach up to 22.82, 17.99, 1.45 and 1.41 times faster than MIP Solver. 2) A Greedy decoding is more time-efficient than a temperature sampling method for the inference process.

VI. CONCLUSION

In this paper, we have investigated the functional split optimization problem in the vRAN system. We have formulated the problem mathematically and analyzed the complexity which is shown to be combinatorial and NP-hard. Finding the exact solution is computationally expensive and therefore, we have proposed a CDRS framework to optimize the locations of functions in vRAN. Because of the large action space and constrained environment of vRAN, we have tailored a policy gradient method with Lagrangian relaxation that uses a penalty signal to lead the policy toward constraint satisfaction. A neural network architecture formed by an encoder-decoder sequence-to-sequence model based on a stacked LSTM network also has been applied to approximate the policy. To avoid the inferred policy suffering from a severe suboptimality, we have leveraged greedy decoding and temperature sampling methods as a search strategy to infer the best solution among candidates from trained models. We also have extensively evaluated our proposed approach in a synthetic network generated by the Waxman algorithm and a real network dataset. The results have shown that CDRS successfully learns the functional split decision with less than 0.05% optimality gap and is the most cost-effective method compared to available RAN setups and has a faster computational time than the optimal baseline solver. It also has shown that altering the routing cost and traffic load does not significantly degrade the optimality. Finally, our proposed approach has shown its effectiveness for solving the functional split optimization offering a near-optimal solution, fast computational time and minimal hand-engineering.

REFERENCES

- [1] F. W. Murti, S. Ali, and M. Latva-aho, "Deep Reinforcement Based Optimization of Function Splitting in Virtualized Radio Access Networks," in *IEEE International Conference on Communications Workshops (ICC Workshops)*, 2021, to appear.
- [2] 3GPP, "Study on new radio access technology: Radio access architecture and interfaces," 3rd Generation Partnership Project (3GPP), Technical Specification (TS) 38.801, 03 2017, version 14.0.0.
- [3] 3GPP, "Architecture description (Release 16)," 3rd Generation Partnership Project (3GPP), Technical Specification Group Radio Access Network (NG-RAN) 38.401, 03 2020, version 16.1.0.
- [4] S. C. Forum, "R6.0. small cell virtualization functional splits and use cases, document 159.07.02," Tech. Rep. Release 7, 2016, version 14.0.0.
- [5] X. Costa-Perez, A. Garcia-Saavedra, X. Li, T. Deiss, A. de la Oliva, A. di Giglio, P. Iovanna, and A. Moored, "5G-Crosshaul: An SDN/NFV Integrated Fronthaul/Backhaul Transport Network Architecture," *IEEE Wireless Communications*, vol. 24, no. 1, pp. 38–45, 2017.
- [6] A. Garcia-Saavedra, J. X. Salvat, X. Li, and X. Costa-Perez, "WizHaul: On the Centralization Degree of Cloud RAN Next Generation Fronthaul," *IEEE Transactions on Mobile Computing*, vol. 17, no. 10, pp. 2452–2466, 2018.

- [7] F. W. Murti, J. A. Ayala-Romero, A. Garcia-Saavedra, X. Costa-Pérez, and G. Iosifidis, "An Optimal Deployment Framework for Multi-Cloud Virtualized Radio Access Networks," *IEEE Transactions on Wireless Communications*, vol. 20, no. 4, pp. 2251–2265, 2021.
- [8] L. M. P. Larsen, A. Checko, and H. L. Christiansen, "A Survey of the Functional Splits Proposed for 5G Mobile Crosshaul Networks," *IEEE Communications Surveys & Tutorials*, vol. 21, no. 1, 2019.
- [9] H. Gupta, M. Sharma, A. Franklin A., and B. R. Tamma, "Apt-RAN: A Flexible Split-Based 5G RAN to Minimize Energy Consumption and Handovers," *IEEE Transactions on Network and Service Management*, vol. 17, no. 1, pp. 473–487, 2020.
- [10] A. Garcia-Saavedra, X. Costa-Perez, D. J. Leith, and G. Iosifidis, "FluidRAN: Optimized vRAN/MEC Orchestration," in *IEEE INFOCOM 2018 - IEEE Conference on Computer Communications*, 2018, pp. 2366–2374.
- [11] A. Garcia-Saavedra, G. Iosifidis, X. Costa-Perez, and D. J. Leith, "Joint Optimization of Edge Computing Architectures and Radio Access Networks," *IEEE Journal on Selected Areas in Communications*, vol. 36, no. 11, pp. 2433–2443, 2018.
- [12] F. W. Murti, A. Garcia-Saavedra, X. Costa-Perez, and G. Iosifidis, "On the Optimization of Multi-Cloud Virtualized Radio Access Networks," in *ICC 2020 - 2020 IEEE International Conference on Communications (ICC)*, 2020, pp. 1–7.
- [13] F. Z. Morais *et al.*, "PlaceRAN: Optimal Placement of Virtualized Network Functions in the Next-generation Radio Access Networks," *IEEE Transactions on Mobile Computing*, 2021, to appear.
- [14] Y. Bengio, A. Lodi, and A. Prouvost, "Machine learning for combinatorial optimization: A methodological tour d’horizon," *European Journal of Operational Research*, vol. 290, no. 2, pp. 405–421, 2021.
- [15] O. Vinyals, M. Fortunato, and N. Jaitly, "Pointer Networks," in *Proceedings of the 28th International Conference on Neural Information Processing Systems - Volume 2*, ser. NIPS’15. MIT Press, 2015, p. 2692–2700.
- [16] I. Bello, H. Pham, Q. V. Le, M. Norouzi, and S. Bengio, "Neural Combinatorial Optimization with Reinforcement Learning," in *International Conference on Learning Representations (ICLR)*.
- [17] R. Solozabal, J. Ceberio, and M. Takáč, "Constrained Combinatorial Optimization with Reinforcement Learning," 2020.
- [18] A. Mirhoseini *et al.*, "Device placement optimization with reinforcement learning," in *Proceedings of the 34th International Conference on Machine Learning*, ser. Proceedings of Machine Learning Research, D. Precup and Y. W. Teh, Eds., vol. 70. PMLR, 06–11 Aug 2017, pp. 2430–2439.
- [19] M. Nazari, A. Oroojlooy, M. Takáč, and L. V. Snyder, "Reinforcement Learning for Solving the Vehicle Routing Problem," in *Proc of NIPS*. Curran Associates Inc., 2018.
- [20] S. Ali *et al.*, "6G White Paper on Machine Learning in Wireless Communication Networks," *ArXiv*, vol. abs/2004.13875, 2020.
- [21] S. Ali, W. Saad, and D. Steinbach, Eds., *White Paper on Machine Learning in Wireless Communication Networks*, ser. 6G Research Visions. Finland: University of Oulu, Jun. 2020, no. 7.
- [22] I. Ahmad *et al.*, "Machine learning meets communication networks: Current trends and future challenges," *IEEE Access*, vol. 8, pp. 223 418–223 460, 2020.
- [23] Q. Jiang, Y. Zhang, and J. Yan, "Neural Combinatorial Optimization for Energy-Efficient Offloading in Mobile Edge Computing," *IEEE Access*, vol. 8, pp. 35 077–35 089, 2020.
- [24] R. Solozabal, J. Ceberio, A. Sanchoyerto, L. Zabala, B. Blanco, and F. Liberal, "Virtual Network Function Placement Optimization With Deep Reinforcement Learning," *IEEE Journal on Selected Areas in Communications*, vol. 38, no. 2, pp. 292–303, 2020.
- [25] J. A. Ayala-Romero, A. Garcia-Saavedra, M. Gramaglia, X. Costa-Perez, A. Banchs, and J. J. Alcaraz, "vrAln: Deep Learning based Orchestration for Computing and Radio Resources in vRANs," *IEEE Transactions on Mobile Computing*, pp. 1–1, 2020.

- [26] S. Matoussi, I. Fajjari, N. Aitsaadi, and R. Langar, “Deep Learning based User Slice Allocation in 5G Radio Access Networks,” in *2020 IEEE 45th Conference on Local Computer Networks (LCN)*, 2020, pp. 286–296.
- [27] R. S. Sutton and A. G. Barto, *Introduction to Reinforcement Learning*, 1st ed. Cambridge, MA, USA: MIT Press, 1998.
- [28] D. Bertsekas, *Nonlinear Programming*. Athena Scientific, 1999.
- [29] Y. Chow, M. Ghavamzadeh, L. Janson, and M. Pavone, “Risk-Constrained Reinforcement Learning with Percentile Risk Criteria,” *Journal of Machine Learning Research*, vol. 18, no. 1, p. 6070–6120, 2017.
- [30] I. Sutskever, O. Vinyals, and Q. V. Le, “Sequence to Sequence Learning with Neural Networks,” in *Proceedings of the 27th International Conference on Neural Information Processing Systems - Volume 2*, ser. NIPS’14. MIT Press, 2014, p. 3104–3112.
- [31] D. Bahdanau, K. Cho, and Y. Bengio, “Neural Machine Translation by Jointly Learning to Align and Translate,” in *International Conference on Learning Representations (ICLR)*, 2015.
- [32] B. Waxman, “Routing of multipoint connections,” *IEEE Journal on Selected Areas in Communications*, vol. 6, no. 9, pp. 1617–1622, 1988.
- [33] S. Orlowski, R. Wessäly, M. Pióro, and A. Tomaszewski, “SNDlib 1.0 Survivable Network Design Library,” 2010.
- [34] M. Mostofa Akbar, M. Sohel Rahman, M. Kaykobad, E. Manning, and G. Shoja, “Solving the Multidimensional Multiple-choice Knapsack Problem by constructing convex hulls,” *Computers and Operations Research*, vol. 33, no. 5, pp. 1259–1273, 2006.
- [35] R. Solozabal, J. Ceberio, and M. Takáč, “Constrained Combinatorial Optimization with Reinforcement Learning,” 2020.
- [36] C. Tessler, D. J. Mankowitz, and S. Mannor, “Reward Constrained Policy Optimization,” in *International Conference on Learning Representations (ICLR)*, 2019.
- [37] S. Orlowski, R. Wessäly, M. Pióro, and A. Tomaszewski, “SNDlib 1.0—Survivable Network Design Library,” *Netw.*, vol. 55, no. 3, p. 276–286, 2010.
- [38] V. Suryaprakash, P. Rost, and G. Fettweis, “Are Heterogeneous Cloud-Based Radio Access Networks Cost Effective?” *IEEE Journal on Selected Areas in Communications*, vol. 33, no. 10, Oct 2015.